ELSEVIER

Corrosion performance of diamond-like carbon (DLC)-coated Ti alloy in the simulated body fluid environment

Ho-Gun Kim[a], Seung-Ho Ahn[a], Jung-Gu Kim[a],*, Se Jun Park[b], Kwang-Ryeol Lee[b]

[a]Department of Advanced Materials Engineering, Sungkyunkwan University, 300 Chunchun-Dong, Jangan-Gu, Suwon 440-746, South Korea
[b]Future Technology Research Division, Korea Institute of Science and Technology, P.O. Box 131, Cheongryang, Sungbuk-Gu, Seoul 130-650, South Korea

Abstract

DLC coatings have been deposited onto substrate of Ti alloy (Ti-6Al-4V) using r.f. PACVD (plasma-assisted chemical vapor deposition) with C_6H_6, and mixture of C_6H_6 and SiH_4 as the process gases. Three kinds of DLC coatings were prepared as a function of diverse bias voltage and Si incorporation. Corrosion performance of DLC coatings was investigated by electrochemical techniques (potentiodynamic polarization test and electrochemical impedance spectroscopy) and surface analyses (atomic force microscopy and scanning electron microscopy). The electrolyte used in this test was a 0.89% NaCl solution of pH 7.4 at temperature 37°C. The porosity and protective efficiency of DLC coatings were obtained using potentiodynamic polarization test. Moreover, the delamination area and volume fraction of water uptake of DLC coatings as a function of immersion time were calculated using electrochemical impedance spectroscopy. This study provides the reliable and quantitative data for assessment of the effect of Si incorporation and an increase of bias voltage on corrosion performance. In conclusion, electrochemical measurements showed that DLC coatings with Si addition and an increase of bias voltage could improve corrosion resistance in the simulated corrosive environment of the body fluid by a 0.89% NaCl solution. This could be attributed to the formation of a dense and low-porosity coating, which impede the penetration of water and ions.
© 2004 Elsevier B.V. All rights reserved.

1. Introduction

The implantation of biomaterials into the human body allows it to increase the quality of life. Biomaterials should have biological and chemical stability to improve functions of the human body. Also, biocompatibility of biomaterials is probably their most important property because biomaterials are used directly or indirectly in contact with the human body. Among the implanted metals used as biomaterials, Ti alloy (Ti-6Al-4V) compared to STS 316L and Co–Cr alloy is extremely similar to bone of the human body. Moreover, Ti alloy has several advantages such as superior biocompatibility and corrosion resistance [1]. However, the overall reaction of the human body on an implant is a system property that includes many different aspects, such as surface chemistry, implant movement, biodegradation and surgical aspects. The highly corrosive environment of the human body restricts the materials to be used for implants [2]. High corrosion resistance is required for the material to use in this corrosive environment [3]. Moreover, wear debris produced from movement of joints can lead to wear-corrosion causing biodegradation [4]. Recently, many researchers have focused on the development of advanced biomaterials to complement these drawbacks. DLC coatings are suitable materials for biomedical application like Ti alloy. DLC coatings have been the subject of extensive investigation in recent years because of its potential of attaining highly desirable properties of technological interest [5]. Many authors have noted the potential of DLC coatings as a protective coating for biomedical applications. DLC coatings have been reported to have

---

* Corresponding author. Tel.: +82 31290 7360; fax: +82 31297 371.
E-mail address: kimjg@skku.ac.kr (J.-G. Kim).

good biocompatibility, such as the absence of inflammatory responses in vitro when assessed by mouse peritoneal macrophages [6] and the absence of histopathological changes in vivo when implanted in animal bone [7]. Furthermore, the unique combination of corrosion resistance, wear resistance, low friction, chemical inertness and electrical insulation make DLC increasingly the preferred candidate for wear-resistant and protective coatings. However, it is difficult to obtain the coatings, which exhibit good adhesion on substrates. Other authors have been informed on the use of amorphous silicon intermediate layer to improve the adhesion of DLC coatings using r.f. PACVD method [8,9].

This study is focused on the evaluation of the electrochemical performance of amorphous hydrogenated carbon (a-C:H) coatings on Ti alloy with amorphous silicon intermediate layer prepared by r.f. PACVD as a function of bias voltage and Si incorporation using electrochemical techniques.

2. Experimental

2.1. Coating deposition

Si-wafer and Ti alloy were used as substrate materials. Samples of 37 mm diameter Ti alloy were cut from a 2-mm-thick sheet. DLC coatings were deposited on mirror-polished substrate and Si-wafer. The sample surfaces were mechanically ground and polished using 2000-grit SiC and 0.3 μm diamond paste for the final step. After cleaning with TCE-aceton-methanol in ultrasonic cleaner sequentially, the polished samples were stored under vacuum. Details of the deposition equipment were previously described elsewhere [10]. A substrate was placed on the water-cooled cathode where 13.56 MHz r.f. power was delivered through the impedance-matching network. In r.f. PACVD method, the vacuum chamber is pumped by a rotary pump and a turbo molecular pump to a base pressure of approximately 2.0×10^{-3} Pa prior to deposition. Before deposition, substrates were precleaned using argon plasma for 15 min at bias voltage of −400 V and pressure of 0.5 Pa. An amorphous Si interlayer of thickness approximately 5 nm is deposited onto the substrate prior to DLC coating for the improvement of adhesion between the coating and substrate. The precursor gas was used as benzene (C_6H_6) for a-C:H films and mixture of C_6H_6 and silane (SiH_4) for the Si–DLC coatings. The coatings were deposited at a bias voltage of −400 or −800 V and deposition pressure of 1.33 Pa. A total coating thickness of about 1 μm was achieved in all cases. The coating thickness was analyzed by alpha-step profilometer. The concentration of Si–DLC coating was controlled to 2 at.% and the composition of Si–DLC coating was measured by Rutherfod backscattering spectroscopy using a collimated $^4He^{2+}$ ion beam of 2 MeV, as shown in Table 1.

Table 1
Composition of coatings analyzed by RBS with deposition conditions

	H (at.%)	C (at.%)	Si (at.%)
Si–DLC Bias voltage(−400 V)	0.215	0.76	0.025
a-C:H Bias voltage(−800 V)	0.18	0.82	0
a-C:H Bias voltage(−400 V)	0.23	0.77	0

2.2. Surface analysis

The SEM investigations were used to examine the surface morphology of the coatings as well as the corroded surfaces of tested specimens. The SEM investigations took place with a voltage of 20 keV.

Surface roughness of coating was analyzed using AFM operated in the contact mode. Information about surface topography was obtained by AFM measurements using microscope of the type Topo Metrix 2010. Images with an area of 1×1 μm were recorded on each surface.

2.3. Electrochemical measurements

Potentiodynamic polarization test was determined with an EG&G Princeton Applied Research Model 273A potentiostat. Potentiodynamic polarization test was carried out in a 0.89% NaCl solution of pH 7.4 at 37°C which was thoroughly deaerated by bubbling high purity nitrogen gas for 0.5 h prior to the immersion of the specimen and continuously purged during the test. This solution was simulated as a human body environment. The exposed coating area was 1 cm^2. Reference and counter electrodes were used for a saturated calomel electrode (SCE) and a pure graphite, respectively. Prior to the beginning of the potentiodynamic polarization test, the specimens were kept in the solution for 6 h in order to establish the open circuit potential (OCP). The potential of the electrode was swept at a rate of 0.166 mV/s from the initial potential of −250 mV versus E_{corr} to the final potential of 1500 mV. The porosity of DLC coating is estimated using electrochemical techniques. Porous coatings cannot prevent the diffusion of aggressive agents through the coating, which lead to delamination of the coating. Even determination of porosity is difficult due to the small size of the defects. By using electrochemical measurements, porosity can be estimated from electrochemical values. Matthes et al. [11] established an empirical equation to estimate the porosity (P) of the coatings:

$$P = \frac{R_{pm(substrate)}}{R_{p(coating-substrate)}} \times 10^{-|\Delta E_{corr}/\beta_a|} \qquad (1)$$

where P was the total coating porosity, R_{pm} the polarization resistance of the substrate and R_p the measured polarization resistance of the coated steel system. ΔE_{corr} is the potential difference between the free corrosion potentials of the coated steel and the bare substrate, and β_a the anodic Tafel slope for the substrate. Also, protective

efficiency (P_i) of the coating was determined from the polarization curve by Eq. (2):

$$P_i = 100\left(1 - \frac{i_{\mathrm{corr}}}{i_{\mathrm{corr}}^{\mathrm{o}}}\right) \tag{2}$$

where i_{corr} and $i_{\mathrm{corr}}^{\mathrm{o}}$ indicate that the corrosion current densities in the presence and absence of the coating, respectively [12].

Electrochemical impedance spectroscopy (EIS) has been frequently used as a non-destructive testing method for assessing the protective performance of coating. Moreover, EIS has been recognized as the powerful instrument to know the surface of the specimens [13]. EIS data were obtained by a Zahner IM6e system using commercial software (THALES) program for AC measurement. Impedance measurements were performed by applying a sinusoidal wave of 10 mV in amplitude to the working electrode at a frequency range from 10 kHz and 10 mHz. The impedance diagrams were interpreted on the basis of the equivalent circuit using THALES fitting program. EIS has been used to determine the amount of delamination and water uptake of coatings exposed to an electrolyte. Thus, the extent of delamination area (A_d) and volume fraction of water uptake (V) could be determined from experimental values of pore resistance (R_{pore}) and coating capacitance (C_{coat}) obtained by the impedance diagrams on the basis of the equivalent circuit [14]. The pore resistance (R_{pore}) of coating is related to the delamination area (A_d), i.e., the pore resistance (R_{pore}) decreases as the delaminated area increases. Therefore, delamination area (A_d) and volume fraction of water uptake (V) available within the coating were calculated by the following equations.

$$A_d = \frac{R_{\mathrm{pore}}^{\mathrm{o}}}{R_{\mathrm{pore}}} \tag{3}$$

$$R_{\mathrm{pore}}^{\mathrm{o}} = \rho \times d\left(ohm \cdot cm^2\right) \tag{4}$$

$$V = \frac{\log[C_{\mathrm{coat}}(t)/C_{\mathrm{coat}}(0)]}{\log 80} \tag{5}$$

where $R_{\mathrm{pore}}^{\mathrm{o}}$ was characteristic value for the corrosion reaction at the solution-coating interface; d, coating thickness; ρ, the coating resistivity; $C_{\mathrm{coat}}(t)$ the coating capacitance as a function of time (t); and $C_{\mathrm{coat}}(0)$, the initial coating capacitance obtained from EIS data at initial exposure.

3. Results and discussion

3.1. Surface analysis

After the completion of potentiodynamic polarization test, the morphology and corrosion features of each substrate and coated system were inspected by S.E.M. and the resulting micrographs are shown in Fig. 1. The surface morphology of DLC coating with Si incorporation and higher bias voltage almost indicated no evidence of penetration of water and ions, as shown in Figs. 1(b) and
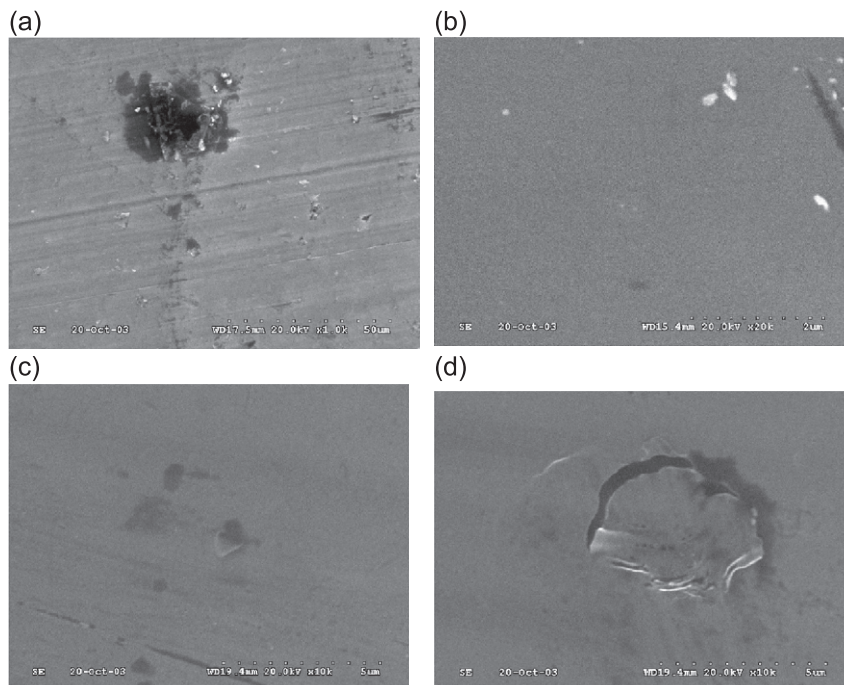

Fig. 1. SEM images showing surface morphologies of DLC coatings after potentiodynamic polarization test; (a) Substrate, (b) Si–DLC, bias voltage=−400 V, (c) a-C:H, bias voltage=−800 V, (d) a-C:H, bias voltage=−400 V.
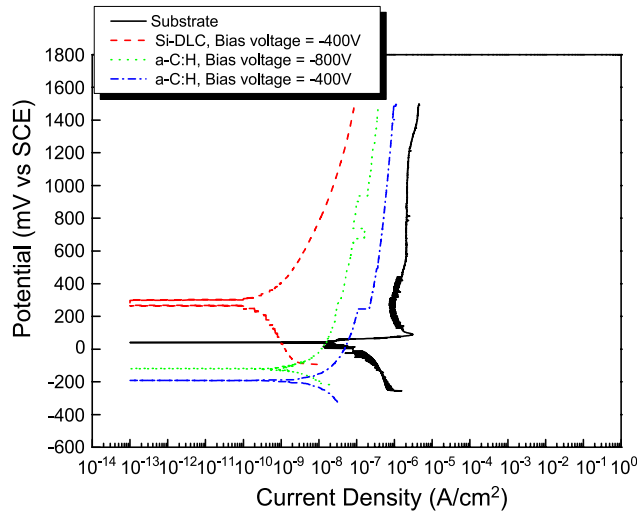
Fig. 2. Potentiodynamic polarization curves in deaerated 0.89% NaCl solution at 37°C (pH=7.4).

(c). The dark part of Fig. 1(d) showed the spots where the coating had flaked off due to penetration of water and ions. The corroded surface morphology confirms the results from the polarization test. This clearly indicates that DLC coatings with Si incorporation and higher bias voltage have excellent corrosion resistance, and no significant damage has been observed.

It is also found that the surface roughness of the specimens with deposited condition. The coating surface roughness of 0.0906 μm for Si–DLC coating, 0.2326 μm for a-C:H (bias voltage=−800 V) and 0.6157 μm for a-C:H (bias voltage=−400 V) was examined through the AFM measurements. This surface roughness is caused by the craters and surface flaws distributed in the outer surface of coating. Thus, the surface becomes smoother and defects decrease with Si incorporation and higher bias voltage. This may importantly affect the contact behavior of the DLC coatings with organic fluid or tissue.

3.2. Electrochemical properties

Potentiodynamic polarization test was carried out in order to investigate the protective abilities of coating. Potentiodynamic polarization curves for DLC coatings in the simulated body fluid environment are shown in Fig. 2. The measured corrosion potential (E_{corr}), corrosion current density (i_{corr}), porosity (P) and protective efficiency (P_i) are given in Table 2. The corrosion current density of

0.04099 nA/cm^2 for Si–DLC coating, 5.477 nA/cm^2 for a-C:H (bias voltage=−800 V) and 51.63 nA/cm^2 for a-C:H (bias voltage=−400 V) was examined. It was seen that the passive region was formed on all the DLC coatings. Especially, Si–DLC coating was well passivated, with low-passive current density and wide passive potential range. It was shown that DLC coatings with Si incorporation and higher bias voltage showed lower corrosion current density than that of a-C:H (bias voltage of −400 V). This means that the coating with fewer pores makes the substrate more passive than the coating with more pores. A combination of the equation of Matthes et al. [11] and the electrochemical determination gives the porosity of 0.284 for a-C:H (bias voltage=−400 V), 0.237 for a-C:H (bias voltage=−800 V) and 0.000043 for Si–DLC (bias voltage=−400 V). This pore can weaken the interfacial material and provide an easy fracture path for metallic ions release. The porosity of DLC coatings with Si incorporation and higher bias voltage is lower than that of a-C:H (bias voltage of −400 V). The lower the calculated porosity, the lower the corrosion current density.

The protective efficiency calculated from corrosion current density was described in Table 2. The protective abilities of coatings increased with increasing the bias voltage and adding Si element into the coatings. The highest protective efficiency was 99.98% of Si–DLC coating. These results are consistent with porosity values. The lower the calculated porosity, the higher the protective efficiency. This is closely related to the corrosion-protective ability and durability of coatings under conditions of applications. As a result, porosity was consistent with protective efficiency.

Interpretation of the EIS measurements is usually done by fitting the impedance data to an equivalent circuit, which is representative of the physical processes taking place in the system under investigation. The electrochemical response to EIS measurements for the DLC coatings was best simulated with the equivalent circuit, as shown in Fig. 3. The equivalent circuit consists of the following elements; R_s corresponds to the solution resistance of the test electrolyte between the working electrode and the reference electrode, and C_{coat} is the capacitance of the coating including pores in the outer layer coating. R_{pore} is the pore resistance resulting from the formation of ionic conduction paths across the coating. C_{dl} is the double layer capacitance of the coating within the pit and R_{ct} is the charge transfer resistance of the coating/substrate interface. Constant phase elements (CPEs) are used in better data fitting to allow for depressed

Table 2
Results of potentiodynamic polarization tests

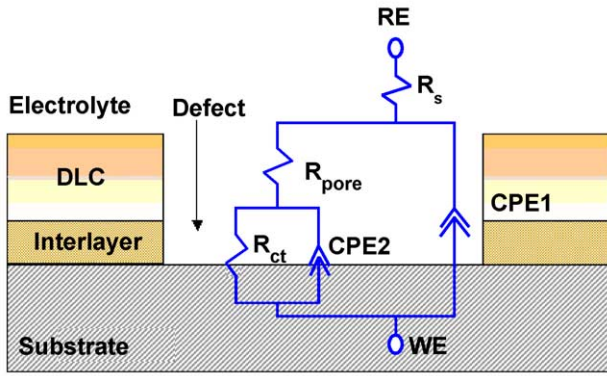| Specimen	E_{corr} (mV)	i_{corr} (nA/cm^2)	β_a (V/decade)	β_c (V/decade)	R_p ($\times 10^3 \, \Omega \, cm^2$)	Protective efficiency (%)	Porosity ($\times 10^{-2}$)
Substrate	−5.48	195.6	0.1142	0.4451	202.2	–	–
Si–DLC Bias voltage(−400 V)	270.6	0.04099	0.2353	0.6027	1795037	99.98	0.000043
a-C:H Bias voltage(−800 V)	−120.2	5.477	0.3608	0.1507	8438.4	97.19	0.237
a-C:H Bias voltage(−400 V)	−193.4	51.63	0.6045	0.2785	1605.5	73.60	0.284

Fig. 3. Equivalent circuit for the DLC coating systems. (WE: working electrode, RE: reference electrode).

semicircles. The capacitances are replaced with CPEs for better fit quality. The CPEs are, in fact, a general expression for many circuit elements. In this paper, C_{coat} and C_{dl} are replaced with CPE1 and CPE2, respectively. The variations of capacitance are indicated in Figs. 4(a) and (b). In the case of a-C:H (bias voltage=−400 V), it is shown that coating capacitance (C_{coat}) increased gradually and water saturates the coating at about 96 h, as shown by the time dependence of coating capacitance. Moreover, double layer capacitance (C_{dl}) of a-C:H (bias voltage=−400 V) increased suddenly at

about 168 h due to permeation of water at coating/substrate interface. This examples showed that water first saturates the coating and simultaneously ionic species pass through the defects of the coating and reach the substrate surface. On the other hand, coating capacitance (C_{coat}) and double layer capacitance (C_{dl}) of DLC coatings with Si incorporation and higher bias voltage show a slight increase or a smaller variations. As shown in Fig. 4(c), it is seen that pore resistance (R_{pore}) of a-C:H (bias voltage=−400 V) decreased after about 96 h because of the continuous diffusion of ionic species within the free volume of the coating. Pore resistance (R_{pore}) of DLC coatings with Si incorporation and higher bias voltage decreased slightly. The coating may swell and increase in number and size of the pores. The decrease of the pore resistance of coating corresponds to the water saturation, as depicted by the increase of coating capacitance in Fig. 4(a). Also, the pore resistance of coating decreases as more ions and water reach the coating surface, causing an increased electrochemical reaction. According to Table 3 and Fig. 4(d), the charge transfer resistance (R_{ct}) decreased with increasing the immersion time. This means that water and ions would have gradually migrated to the substrate surface. The values of R_{ct} with Si incorporation and higher bias voltage are higher than that of a-C:H (bias voltage=−400 V), as presented in Fig. 4(d). It is important that the high R_{ct}
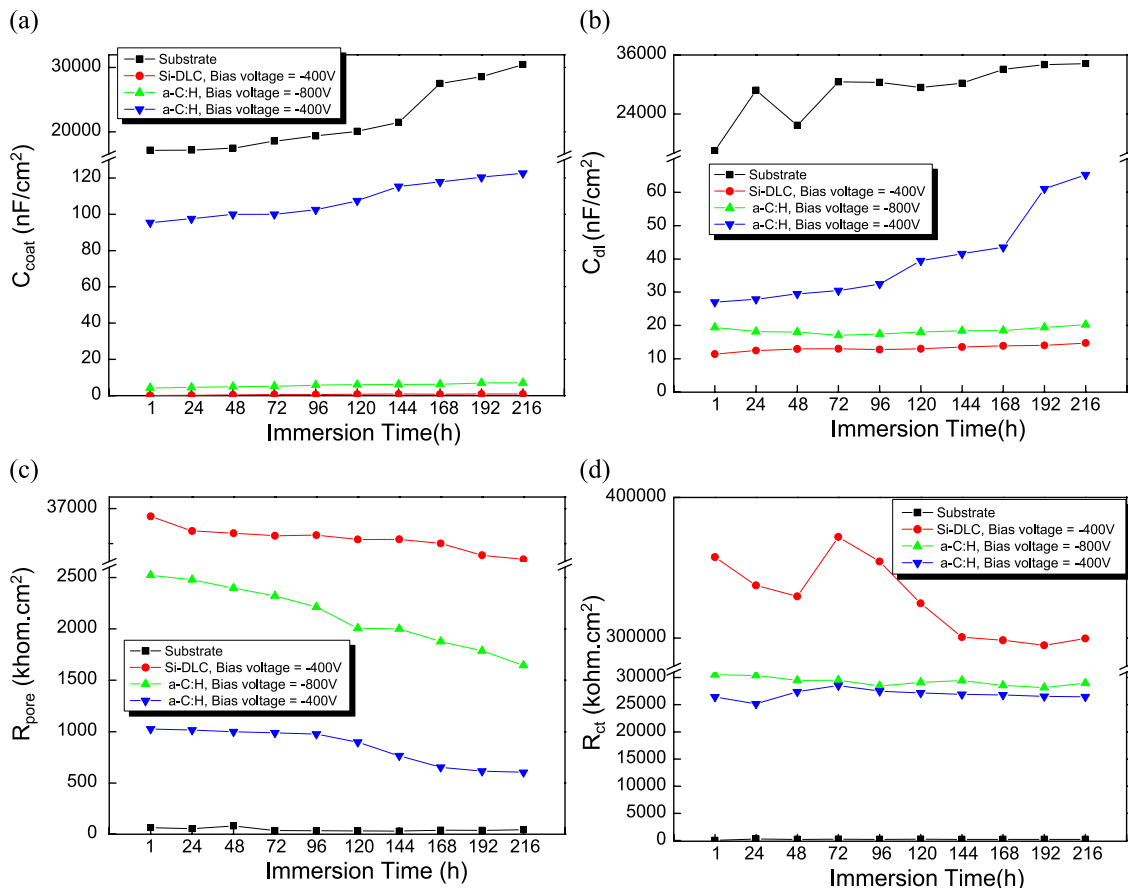

Fig. 4. (a) Coating capacitance, (b) double layer capacitance, (c) pore resistance and (d) charge transfer resistance as a function of immersion time.

Table 3
Result of electrochemical impedance spectroscopy measurements

Exposure time		R_s (Ω cm^2)	CPE1		R_{pore} ($\times 10^3$ Ω cm^2)	CPE2		R_{ct} ($\times 10^3$ Ω cm^2)	A_d ($\times 10^{-4}$)	V
			C_{coat} ($\times 10^{-9}$ F/cm^2)	n (0–1)		C_{dl} ($\times 10^{-9}$ F/cm^2)	n (0–1)			
1 h	Substrate	2541	17,090	0.9381	65.6	16,470	1	297.1	–	–
	Si–DLC (−400 V)	28,380	0.136	0.8977	34,890	11.42	1	357,600	0.00041	0.76
	a-C:H (−800 V)	1245	4.332	0.8545	2524	19.42	1	30,540	0.35	1.89
	a-C:H (−400 V)	1172	95.42	0.8847	1027	26.98	1	26,450	1.61	2.65
96 h	Substrate	8543	19,340	1	34.4	30,420	1	316.3	–	–
	Si–DLC (−400 V)	17,540	0.624	0.9047	29,987	12.78	1	354,400	0.00047	1.11
	a-C:H (−800 V)	2544	5.876	0.9017	2214	17.47	1	28,470	0.40	1.96
	a-C:H (−400 V)	4572	102.47	0.8859	976	32.44	1	27,520	1.69	2.66
216 h	Substrate	1734	30,470	1	44.61	34,250	1	253.4	–	–
	Si–DLC (−400 V)	24,540	0.897	0.8994	23,569	14.72	1	299,700	0.00060	1.19
	a-C:H (−800 V)	1988	7.014	0.8499	1644	20.24	1	28,990	0.54	2.00
	a-C:H (−400 V)	3514	122.59	0.8909	604	65.25	1	26,490	2.73	2.71

value indicates good corrosion resistance. Consequently, it was shown that corrosion resistance of DLC coatings with Si incorporation and higher bias voltage would be improved in corrosive environment.

Also, the results obtained from EIS measurements were usually used to monitor the change of delamination area (A_d) and volume fraction of water uptake (V). Figs. 5 and 6 show delamination area (A_d) and volume fraction of water uptake (V) of three kinds of DLC coatings, respectively. After a constant value of delamination area during the 96 h immersion, a-C:H (bias voltage=−400 V) shows a sudden increase, as shown in Fig. 5. On the other hand, delamination area with Si incorporation and higher bias voltage indicates a slight decrease or stabilization for increasing immersion time. Delamination area was affected by the volume fraction of water uptake through porous coating because penetration of water in coating led to delamination and blisters. It is seen that longer time of exposure leads to a continuous increase of the volume fraction of water uptake, as shown in Fig. 6. Especially, the volume fraction of water uptake of a-C:H (bias

voltage=−400 V) tends to absorb more water due to the enhancement of diffusion mechanisms of active species through the coating. Consequently, delamination area and the volume fraction of water uptake with Si incorporation and higher bias voltage are much lower than those of a-C:H (bias voltage=−400 V), as shown in Figs. 5 and 6. It is clear that delamination area and volume fraction of water uptake with Si incorporation and higher bias voltage absorb less amount of water compared to a-C:H (bias voltage=−400 V).

The excellent agreement between the delamination area and the volume fraction of water uptake over the test period suggests that porosity is indeed strongly related to the coating delamination and the fraction of the substrate which is wetted by the electrolyte through defects. Moreover, small structural defects, e.g., pinholes, pores and cracks, act as channels for the corrosion of the substrate. The porosity of coating is the main cause of coating delamination. Thus, delaminated area was influenced by the porosity because the lager the amount of porosity, the larger the delaminated area.
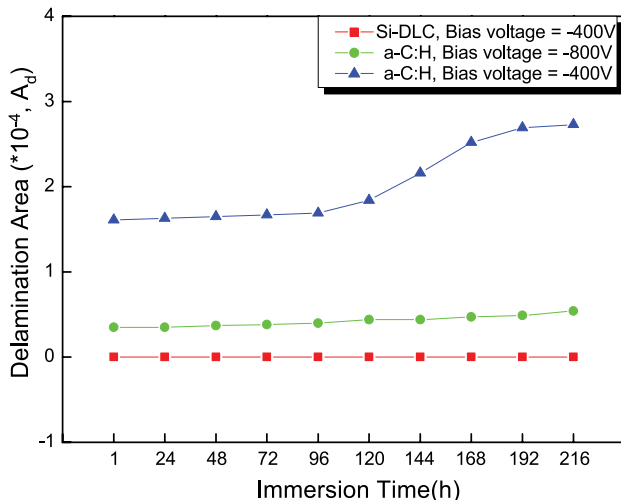

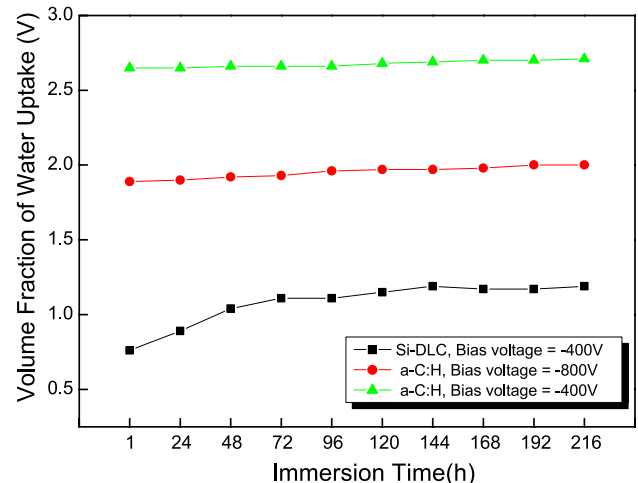
Fig. 5. Delamination area as a function of immersion time.

Fig. 6. Volume fraction of water uptake as a function of immersion time.

4. Conclusions

(1) DLC coatings with Si incorporation and higher bias voltage showed lower corrosion current density and porosity than a-C:H (bias voltage=−400 V), indicating better corrosion resistance.

(2) An increase of bias voltage and Si incorporation reduced delamination area (A_d) and volume fraction of water uptake (V) in DLC coatings. Also, charge transfer resistance (R_{ct}) values with Si incorporation and higher bias voltage were increased.

(3) From the SEM and AFM images, the pitting corrosion of DLC coatings as an increase of bias voltage and addition of Si element was not as severe as those of other coatings, and the surface becomes smoother and defects decrease with Si incorporation and higher bias voltage, respectively.

Acknowledgements

References

[1] H. Matsuno, A. Yokoyama, F. Watari, M. Uo, T. Kawasaki, Biomaterials 22 (2001) 1253.
[2] R. Hauert, Diamond Relat. Mater. 12 (2003) 583.
[3] Y. Hayashi, G. Nakayama, Corros. Sci. Technol. 1 (2002) 491.
[4] H. Kim, J.J. Lee, J. Kor. Inst. Met. Mater. 16 (2003) 11.
[5] P. Papakonstantinou, J.F. Zhao, P. Lemoine, E.T. McAdams, J.A. McLaughlin, Diamond Relat. Mater. 11 (2002) 1074.
[6] L.A. Thomson, F.C. Law, N. Rushton, J. Franks, Biomaterials 12 (1991) 37.
[7] D.P. Dowling, P.V. Kola, K. Donnelly, T.C. Kelly, K. Brumitt, L. Lloyd, R. Eloy, M. Therin, N. Weill, Diamond Relat. Mater. 6 (1997) 390.
[8] L. Chandra, M. Allen, R. Butter, N. Rushton, A.H. Lettington, T.W. Clyne, Diamond Relat. Mater. 4 (1995) 852.
[9] R. Butter, M. Allen, L. Chandra, A.H. Lettington, N. Rushton, Diamond Relat. Mater. 4 (1995) 857.
[10] K.-R. Lee, M.-G. Kim, S.-J. Cho, Y. Eun, T.-Y. Seong, Thin Solid Films 308 (1997) 263.
[11] B. Matthes, E. Brozeit, J. Aromaa, H. Ronkainen, S.P. Hannula, A. Leyland, A. Matthews, Surf. Coat. Technol. 49 (1991) 489.
[12] Y.J. Yu, J.G. Kim, S.H. Cho, J.H. Boo, Surf. Coat. Technol. 162 (2003) 161.
[13] T.H. Ha, D.K. Kim, J.H. Bae, H.G. Lee, S.J. Lee, Corros. Sci. Technol. 1 (2002) 444.
[14] F. Mansfeld, C.H. Tsai, Corrosion 49 (1993) 727.